ISSN: 1305-130X
e-ISSN: 1305-1385
Celal Bayar University Journal of Science
2026; 22 (3); 475-486

Electronic Properties and Crystal Packing Interactions in Bismuth(III) Iodide Thioamide Complexes: A Combined DFT and Hirshfeld Surface Study

Okan Ucar[1] , Ibrahim Ismet Ozturk[2]

ABSTRACT

A series of experimentally characterized complexes were selected from the literature to determine the electronic properties, energy levels, and to investigate the formation of the crystal lattice of bismuth(III) halide complexes. In this study, emphasis was placed on the parameters of E_{HOMO} (Highest Occupied Molecular Orbital energy), E_{LUMO} (Lowest Unoccupied Molecular Orbital energy), energy gap (ΔE), chemical hardness (η), absolute electronegativity (χ), and electrophilicity (ω) for monomeric, dimeric, and polymeric bismuth(III) halide complexes. Comparison of the HOMO energy levels revealed that complex 1 possesses a higher electron-donating potential. The LUMO energy levels indicated that the monomeric unit of the polymeric structure (complex 3) is more prone to electron acceptance. Furthermore, according to the data obtained from Hirshfeld surface analysis, hydrogen bonding interactions were found to contribute most significantly to the formation of the crystal structures.

Keywords: *Bismuth(III) Iodide, Thioamide, DFT, HOMO-LUMO, Hirshfeld Surfaces.*

1. INTRODUCTION

Bismuth is an element belonging to the pnictogen group and is commonly found in compounds exhibiting +3 and +5 oxidation states [1–3]. The presence of the $6s^2$ electron pair in the electron configuration of the Bi(III) ion allows for non-ideal molecular geometries and wide band gaps [4–7] This feature leads to rich structural diversity in bismuth compounds. In addition to its significance in coordination chemistry, bismuth has been widely used in the medical field for many years due to its non-toxic nature [8–10]. Historically, bismuth oxide was used for wound healing in the 18th century [11,12]. Subsequently, bismuth-containing pharmaceuticals such as sodium bismuth tartrate and bismuth subsalicylate were developed [13,14]. Today, research and development studies on bismuth continue for the treatment of various diseases [15,16].

[1] Corresponding Author: okanucar@nku.edu.tr
[1] Section of Analytical Chemistry, Department of Chemistry, Yozgat Bozok University, 66100, Yozgat, Türkiye, 0000-0001-5921-3324
[2] Section of Inorganic Chemistry, Department of Chemistry, Faculty of Arts and Sciences, Tekirdag Namik Kemal University, 59030 Tekirdag, Türkiye, 0000-0003-3164-0038

Article Submission Date: April 6, 2026 / Acceptance Date: June 16, 2026
Doi Number: 10.18466/cbayarfbe.1924290
Article Type: Research Article

One of the factors influencing the molecular geometries of bismuth(III) complexes is the type of ligand [17,18]. Various molecular geometries have been reported for bismuth(III) halide complexes containing thioamide-derived ligands [19,20]. In these complexes, which may exist in monomeric, dimeric, or polymeric forms, the coordination number is typically six, and the geometry is most often completed to an octahedral arrangement [21]. Bi-X (X: halogen atom) and Bi-S (S: donor atom from the thioamide ligand) bridging bonds enable the linkage of monomeric units, thereby facilitating dimerization or polymerization [22–24].

In this study, experimental data for three different complexes formed between the heterocyclic thioamide ligands 2-mercapto-3,4,5,6-tetrahydropyrimidine, 2-mercaptobenzimidazole, and 2-mercapto-1-methylimidazole and bismuth(III) iodide were obtained from the literature (Figure 1) [25]. The bismuth(III) iodide complex of 2-mercapto-3,4,5,6-tetrahydropyrimidine exists as a monomer (complex 1), the complex of 2-mercaptobenzimidazole forms a dimeric structure (complex 2), and the complex of 2-mercapto-1-methylimidazole exhibits a polymeric structure. The differences in electronic properties and intermolecular interactions among these complexes, which possess similar ligand frameworks but distinct structural motifs, were systematically investigated. For this purpose, the Density Functional Theory (DFT) method and Hirshfeld surface analysis were employed.

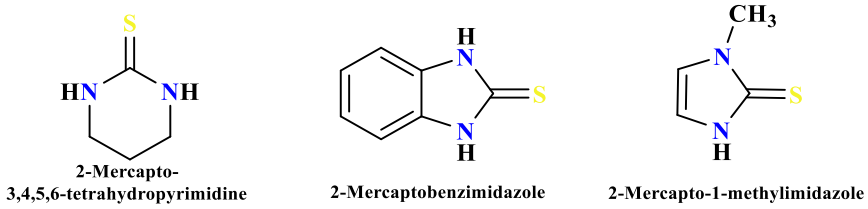


Figure 1. The molecular structures of the thioamide ligands in bismuth(III) halide complexes.

Although the selected bismuth(III) iodide complexes have previously been synthesized and structurally characterized, a comparative investigation of their electronic structures and crystal-packing interactions using a combined DFT and Hirshfeld surface approach has not been reported so far. The coexistence of monomeric, dimeric, and polymeric architectures within a chemically related family of bismuth(III) complexes provides a unique opportunity to examine how structural organization influences electronic properties and intermolecular interactions. Therefore, the present study aims to establish structure–property relationships by systematically comparing the frontier molecular orbital characteristics, quantum chemical parameters, charge distributions, and crystal-packing features of these complexes. The findings contribute to a deeper understanding of the factors governing the electronic behavior and supramolecular assembly of bismuth(III) iodide–thioamide systems.

2. MATERIALS AND METHODS

The electronic properties of the complexes were investigated using Density Functional Theory (DFT) calculations performed with Gaussian 16 and visualized using GaussView 6.0.16. For the determination of frontier molecular orbitals and energy values, the B3LYP functional together with the LanL2DZ basis set was employed for the bismuth(III) complexes. The B3LYP hybrid functional was selected because of its proven reliability in describing the structural and electronic properties of coordination compounds. For the Bi(III) center, the LanL2DZ basis set was employed since it incorporates an effective core potential (ECP), allowing an efficient treatment of relativistic effects and core electrons while maintaining a reasonable computational cost. Furthermore, the B3LYP/LanL2DZ level has been successfully applied in previous studies on heavy main-group metal complexes, providing results consistent with experimental observations. The CIF files related to the crystal data of the complexes were obtained from the reported study in the literature [25]. The quantum parameter data were obtained using formulas from the literature [26].

Furthermore, intermolecular interactions present in the crystal lattice of the bismuth(III) complexes were qualitatively and quantitatively analyzed using Hirshfeld Surface analysis based on the same CIF files. The Hirshfeld Surface analysis was carried out using the Crystal Explorer 21.5 software.

3. RESULTS AND DISCUSSIONS

The geometric optimizations of bismuth(III) iodide complexes were carried out using the LanL2DZ basis set in the Gaussian View 6.0.16 program (Figure 2). It is necessary to verify that the optimized geometries correspond to true minima on the potential energy surface. For this purpose, frequency calculations were performed at the same level of theory following the geometry optimizations. No imaginary frequencies were detected in the calculated vibrational spectra. These results confirm that all optimized structures correspond to true minima on the potential energy surface.

The energy values of the frontier molecular orbitals were utilized to investigate the molecular properties (Figure 3). The higher HOMO energy value of complex 1 in the monomeric structure compared to the others indicates a greater electron-donating ability. Accordingly, this monomeric complex exhibits a higher nucleophilic character. In contrast, complex 3 with a polymeric structure possesses a lower LUMO energy, which enhances its electron-accepting capability. The negative frontier orbital energy values of the complexes indicate their high stability. Among these three complexes, complex 3, which has the smallest energy gap, is less stable and exhibits higher reactivity. This behavior may be associated with the tendency of the monomeric units to form an extended polymeric network.

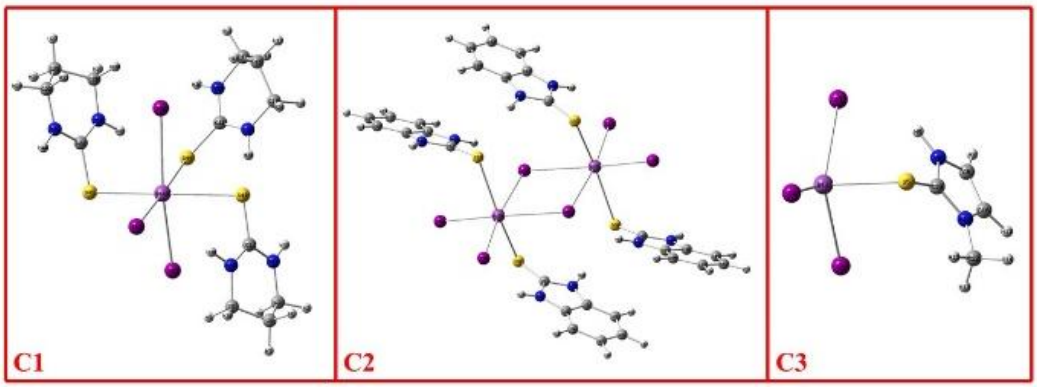


Figure 2. Optimized molecular structures of bismuth(III) iodide–thioamide complexes (B3LYP, LanL2DZ).

The chemical hardness values of the complexes are 1.85 eV, 1.78 eV, and 1.54 eV, respectively. Chemical hardness represents the resistance to charge transfer and is inversely proportional to chemical softness. According to the values presented in Table 1, complex 1 exhibits the greatest resistance to charge transfer, whereas complex 3, which has the highest softness value, allows greater charge transfer, thereby increasing its reactivity [27]. Another important parameter is electrophilicity. It is observed that the electrophilicity value increases with the degree of polymerization of the structure. Since electrophilicity increases depending on the electron-withdrawing ability, it is consistent with electronegativity, and both of these values are highest for complex 3 [28].

A comparison of complexes 1–3 reveals a clear relationship between the degree of aggregation and the electronic properties. While the monomeric complex 1 exhibits the highest HOMO energy and the largest HOMO–LUMO energy gap, the polymeric complex 3 possesses the lowest LUMO energy and the smallest energy gap. The dimeric complex 2 displays intermediate characteristics. This trend suggests that increasing structural aggregation is accompanied by enhanced electron-accepting ability, reduced chemical hardness, and increased chemical reactivity. These observations indicate that structural organization plays an important role in determining the electronic behavior of bismuth(III) iodide–thioamide complexes.

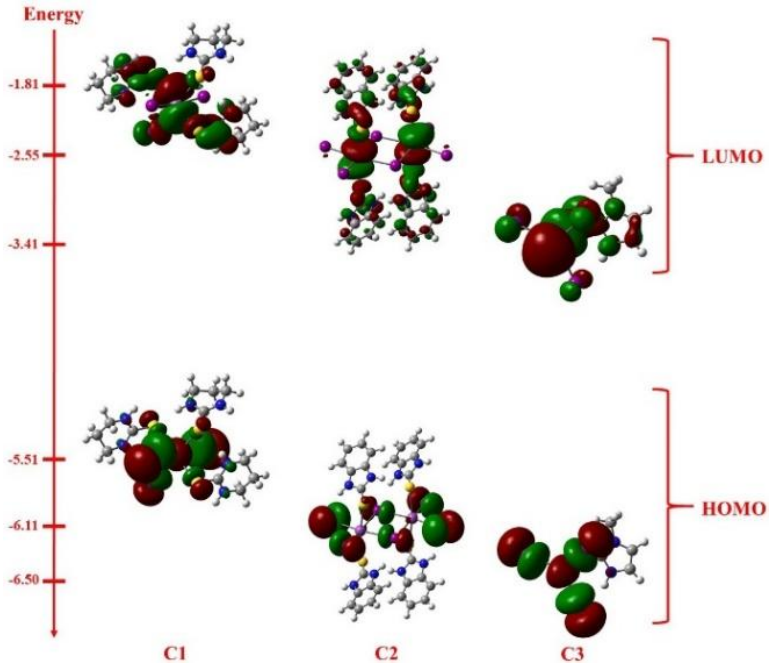


Figure 3. HOMO and LUMO electron density distributions and corresponding frontier molecular orbital energy levels of bismuth(III) complexes 1–3.

Atomic charge distribution and electron density provide important insights into the physicochemical properties of molecular systems. These charges are commonly used as indicators of chemical reactivity or as measures of weak intermolecular interactions. The atomic charges of chemical species also provide insight into the molecular polarity. The Mulliken charge distribution method is a key computational approach in Gaussian for obtaining this information. The results of the Mulliken charge distribution calculations are shown in Figure 4. In the figure, green represents positive charges, whereas red indicates negative charges, with increasing color intensity corresponding to higher charge magnitude. In all complexes, the largest positive charge is localized around the bismuth(III) ion. The net charge of the bismuth ion, originally +3, shifts to values between −0.720 and −0.770 upon complex formation, which is attributed to electron transfer from the ligands to the central ion. As expected, the negative charge is higher on the halogen atoms. Among the iodine atoms, those bridging between bismuth(III) ions carry higher negative charges compared to the terminal iodine atoms.

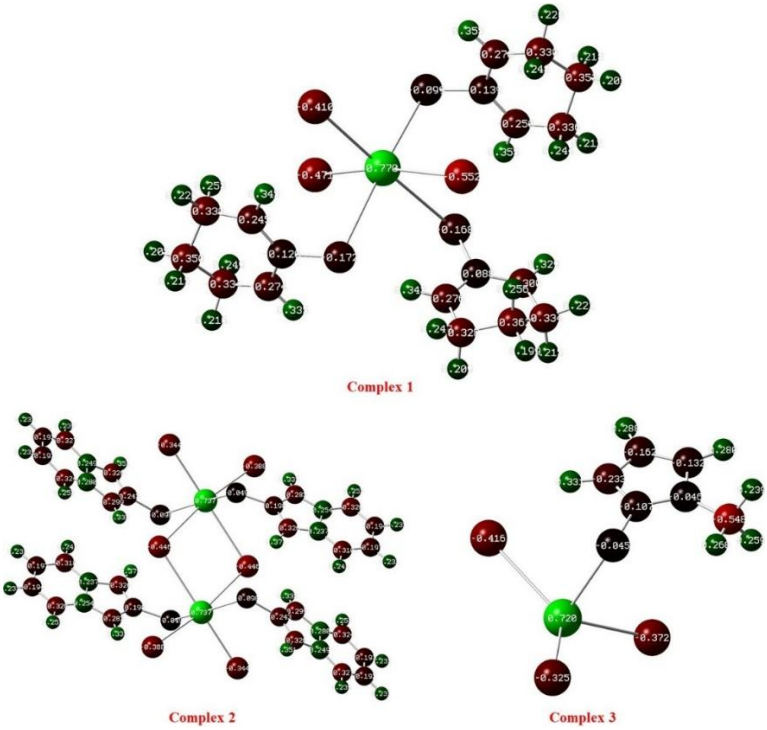


Figure 4. Mulliken atomic charge distributions of bismuth(III) complexes 1–3.

Table 1. The quantum parameters of bismuth(III) complexes 1-3 (eV).

Compounds	E_{HOMO}	E_{LUMO}	ΔE	IP	EA	μ	η	χ	ω
Complex 1	-5.51	-1.81	3.70	5.51	1.81	-3.66	1.85	3.66	3.62
Complex 2	-6.11	-2.55	3.56	6.11	2.55	-4.33	1.78	4.33	5.27
Complex 3	-6.50	-3.41	3.09	6.50	3.41	-4.95	1.54	4.95	7.94

The Hirshfeld surface analysis was performed to determine the types of interactions present in the crystal lattice of bismuth(III) iodide thioamide complexes. From the Hirshfeld surface analysis, the d_{norm}, d_e, and d_i maps (Figure 5), as well as the shape index, curvedness, and fragment patch maps (Figure 6), were generated for the complexes. The d_{norm} (normalized contact distance) is calculated using the d_i (internal) and d_e (external) distances, and the equation given below is employed [29].

$$d_{norm} = \frac{d_i - r_i^{vdw}}{r_i^{vdw}} + \frac{d_e - r_e^{vdw}}{r_e^{vdw}} \quad \textbf{(3.1)}$$

r_i^{vdw} and r_e^{vdw} represent the van der Waals radii of the atoms inside and outside the surface, respectively. White, blue, and red colors are used in the dnorm maps. The red color indicates close contact distances, the white color represents contacts with distances approximately equal to the van der Waals radii, and the blue color corresponds to interactions with longer contact distances [30].

The resolution scales for the Hirshfeld maps are as follows:

d_{norm}: -0.3804 to 1.6773 Å (1), -0.2942 to 3.1395 Å (2), -0.3595 to 1.1544 Å (3);

d_e: 0.8576 to 3.2288 Å (1), 0.9136 to 4.9097 Å (2), 0.8753 to 2.9387 Å (3);

d_i: 0.8586 to 2.9469 Å (1), 0.9138 to 3.9434 Å (2), and 0.8756 to 3.0310 Å (3).

These resolution values are identical for all complexes in the shape index (-1.0 to 1.0 Å), curvedness (-4.0 to 0.4 Å), and fragment patch (0.0 to 19.0 Å) maps.

In the d_{norm} map of complex 1, short S···H/H···S and I···H/H···I interactions are represented by red regions. In complex 2, S···H/H···S, H···H, and C···C interactions, and in complex 3, Bi···I/I···Bi and I···H/H···I interactions are shorter than the van der Waals radii and correspond to red spots (Figure 7). These strong interactions are generally attributed to hydrogen bonding. For complex 3, which has a polymeric structure, the Bi–I–Bi linkages responsible for polymerization are also observed as strong interactions in the d_{norm} map.

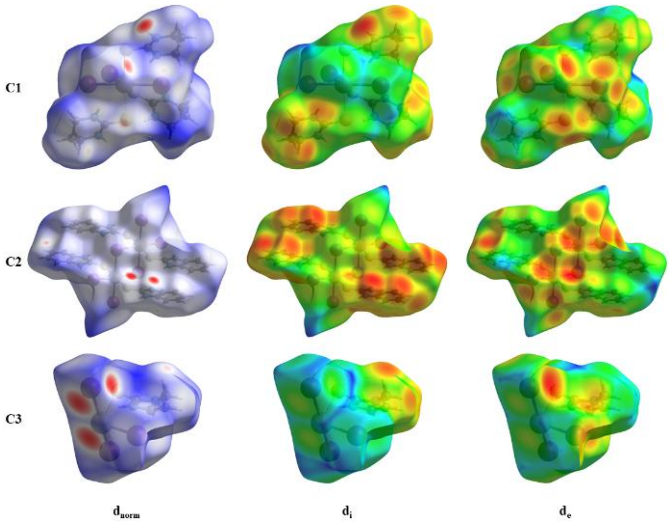


Figure 5. Hirshfeld surface maps (d_{norm}, d_e, and d_i) of bismuth(III) complexes 1–3 showing intermolecular contact regions within the crystal structures.

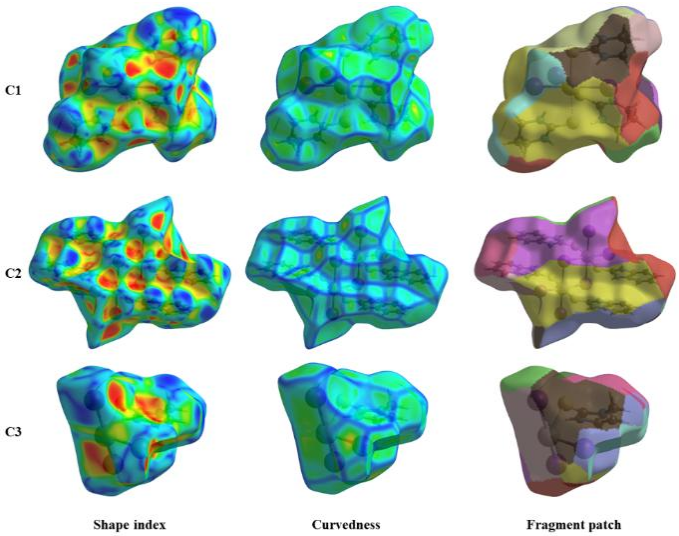


Figure 6. Shape index, curvedness, and fragment patch maps of bismuth(III) halide complexes 1-3.

The quantitative contributions of the interactions that hold the crystal lattice together can be determined using two-dimensional (2D) fingerprint plots (Figure 8) [31]. In complex 1, the interaction contributing the most to the structure is the H···H interaction (44.5%). This is followed by I···H/H···I (31.8%) and S···H/H···S (17.0%) interactions. A similar trend is observed in complex 2. The interactions contributing most to the crystal lattice are, in order, I···H/H···I (49.8%), H···H (18.7%), and S···H/H···S (13.9%). In complex 3, following the I···H/H···I (43.6%) and H···H (12.7%) interactions, the Bi···I/I···Bi interaction (12.1%), which is also effective in the formation of the polymeric chain, is observed.

Comparison of the fingerprint plots demonstrates that the dominant intermolecular interactions vary considerably with structural architecture. While H···H contacts constitute the major contribution to the crystal packing of the monomeric complex 1, I···H/H···I interactions become increasingly dominant in the dimeric and polymeric complexes. Furthermore, the appearance of Bi···I/I···Bi contacts exclusively in complex 3 directly reflects the polymeric nature of the structure and highlights the role of metal–halide bridging interactions in directing supramolecular assembly. These findings indicate that the crystal packing characteristics are strongly influenced by the aggregation mode of the complexes.

The Hirshfeld surface results are consistent with the DFT calculations. The polymeric complex 3, which exhibits the smallest HOMO–LUMO energy gap and the highest

softness, also displays the most diverse intermolecular interaction pattern, including significant Bi···I contacts. This correlation suggests that increased electronic flexibility may facilitate the formation of extended supramolecular architectures and stronger crystal-packing interactions.

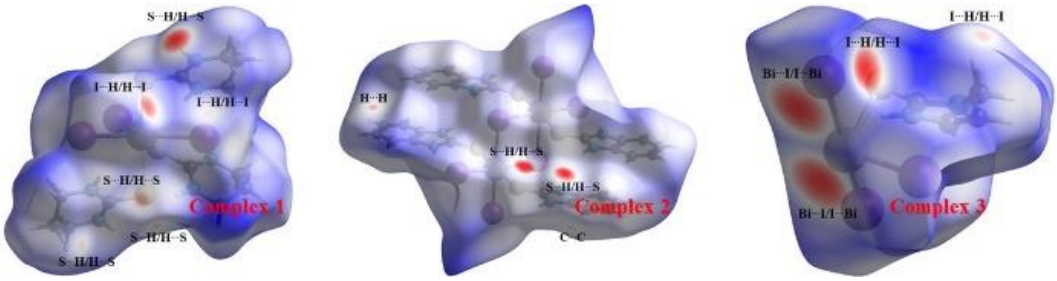


Figure 7. Significant interactions in the d_{norm} maps of bismuth(III) halide complexes 1-3.

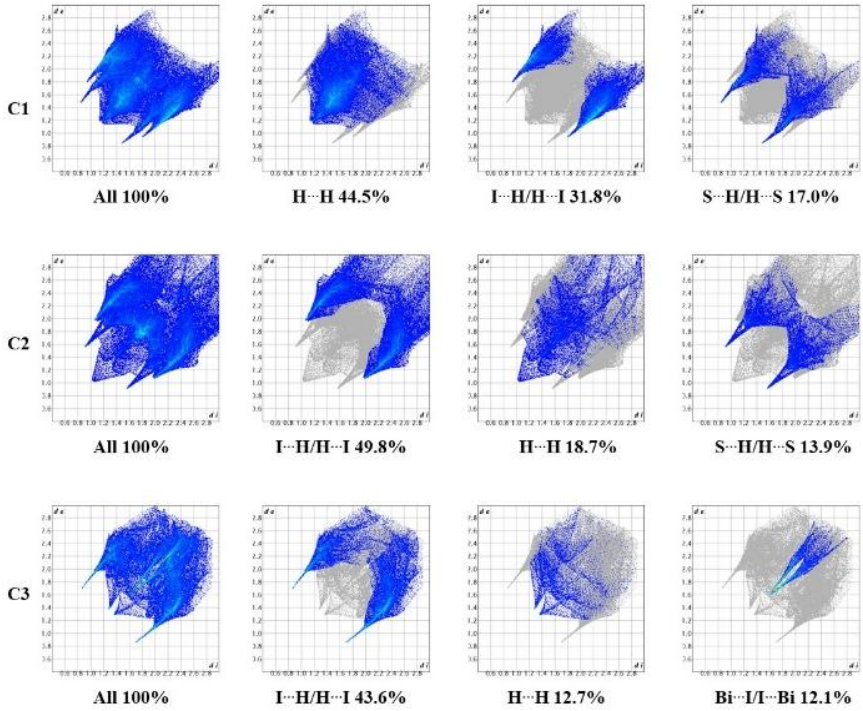


Figure 8. Percentages of the contacts with the highest contributions obtained from the fingerprint plots of complexes 1-3.

4. CONCLUSION AND RECOMMENDATIONS

In this study, theoretical investigations were carried out on three bismuth(III) iodide–thioamide complexes existing in monomeric, dimeric, and polymeric forms. Density Functional Theory (DFT) calculations provided information about the optimized coordination geometries, quantum chemical parameters, and reactivity properties of the complexes. In particular, the relatively small energy gap between the frontier molecular orbitals and the lower stability of the monomeric unit within the polymeric complex was found to enhance molecular reactivity. This behavior indicates a pronounced tendency of the structure toward polymerization. In contrast, the low reactivity of complex 1, which does not form any dimeric or polymeric structure, further supports the reliability of the obtained results. Moreover, it was observed that hydrogen bonding interactions play a significant role in determining the stability of the crystal structure.

Beyond the specific findings obtained for the investigated complexes, this study contributes to coordination chemistry by demonstrating how different structural architectures, namely monomeric, dimeric, and polymeric organizations, influence the electronic properties and intermolecular interactions of bismuth(III) iodide–thioamide complexes. The combined application of DFT calculations and Hirshfeld surface analysis provides a comprehensive framework for correlating structural organization with electronic behavior and crystal-packing characteristics. These findings contribute to a better understanding of structure–property relationships in main-group metal complexes and may provide useful guidance for future theoretical and experimental studies in this field.

Research and Publication Ethics Statement

There are no ethical issues after the publication of this manuscript.

Author's Contributions

Okan Ucar: Prepared the draft and the text; conducted a portion of the theoretical work.

Ibrahim İsmet Ozturk: They carried out work involving article writing and theoretical study processes.

REFERENCES

[1]. Gowda, V, Sarma, B, Laitinen, RS, Larsson, AC, Ivanov, AV, Iuga, D, Lantto, P, Antzutkin, ON. 2017. Structural insights into the polymorphism of bismuth(III) di-n-butyldithiocarbamate by X-ray diffraction, solid-state ($^{13}C/^{15}N$) CP-MAS NMR and DFT calculations. *Polyhedron*; 129: 123-132.

[2]. Kearns, J, Turner, A. 2016. An evaluation of the toxicity and bioaccumulation of bismuth in the coastal environment using three species of macroalga. *Environ Pollut*; 208: 435-441.

[3]. Sivasekar, S, Ramalingam, K, Rizzoli, C, Alexander, N. 2014. Synthesis, structural, continuous shape measure and bond valence sum characterization of bismuth(III) complexes of substituted dithiocarbamates and their solvothermal decomposition. *Inorgan Chim Acta*; 419: 82-88.

[4]. Yang, Y, Ouyang, R, Xu, L, Guo, N, Li, W, Feng, K, Yang, Z, Zhou, S, Miao, Y. 2015. Review: bismuth complexes: synthesis and applications in biomedicine. *J Coord Chem*; 68(3): 1-19.

[5]. Li, YK, Yang, M, Li, MX, Yu, H, Wu, HC, Xie, SQ. 2013. Synthesis, crystal structure and biological evaluation of a main group seven-coordinated bismuth(III) complex with 2-acetylpyridine N4-phenylthiosemicarbazone. *Bioorg Med Chem Lett*; 23: 2288-2292.

[6]. Shetu, SA, Sanchez-Palestino, LM, Rivera, G, Bandyopadhyay, D. 2022. Medicinal bismuth: bismuth-organic frameworks as pharmaceutically privileged compounds. *Tetrahedron*; 129: 133117.

[7]. Toumi, E, Elleuch, N, Shova, S, Boujelbene, M. 2025. Investigation of vibrational, Hirshfeld surface and optical properties of a new semi-conductor hybrid based on Bi(III) and 2-methylimidazole. *J Mol Struct*; 1338: 142222.

[8]. Beltrán-Torres, M, Santacruz-Ortega, H, López-Gastelum, KA, Acosta-Elías, M, Velázquez-Contreras, EF, Aguirre-Hernández, G, Hernández-Paredes, J, Pérez-González, R, Rocha-Alonzo, F, García-Galaz, A, Sugich-Miranda, R. 2024. Synthesis via microwave irradiation, structural characterization, and antibacterial activities of new complexes of bismuth(III) with thiosemicarbazones. *Polyhedron*; 252: 116883.

[9]. Ozturk, II, Gurgan, ES. 2022. Synthesis, characterization, anti-bacterial and anti-inflammatory activities of bismuth(III) complexes based on 5-chloro-2-mercaptobenzothiazole. *Hittite J Sci Eng*; 9: 225-233.

[10]. Beniwal, S, Gaur, S, Sharma, J. 2022. Syntheses and characterization of some homodimer complexes of bismuth(III) having a Bi…Bi linkage along with molecular modeling, antimicrobial, antioxidant and cytotoxic studies. *J Coord Chem*; 75: 3000-3014.

[11]. Keogan, D, Griffith, D. 2014. Current and potential applications of bismuth-based drugs. *Molecules*; 19: 15258-15297.

[12]. Hassan, M, Diab, MA, Abd El-Wahab, MG, Hegazi, AH, Emwas, AH, Jaremko, M, Hagar, M. 2023. Bismuth oxide composite-based agricultural waste for wound dressing applications. *Molecules*; 28: 5900.

[13]. Duffin, RN, Werrett, MV, Andrews, PC. 2020. Antimony and bismuth as antimicrobial agents. *Elsevier Inc*.

[14]. Arda, M, Ozturk, II, Banti, CN, Kourkoumelis, N, Manoli, M, Tasiopoulos, AJ, Hadjikakou, SK. 2016. Novel bismuth compounds: synthesis, characterization and biological activity against human adenocarcinoma cells. *RSC Adv*; 6: 29026-29044.

[15]. Turk, K, Grześkiewicz, AM, Banti, CN, Hadjikakou, SK, Kubicki, M, Ozturk, II. 2022. Synthesis, characterization, and biological properties of mono-, di- and poly-nuclear bismuth(III) halide complexes containing thiophene-2-carbaldehyde thiosemicarbazones. *J Inorg Biochem*; 237: 111987.

[16]. Ozturk, II, Turk, K, Grześkiewicz, AM, Kubicki, M, Banti, CN, Hadjikakou, SK. 2023. Heteroleptic six-coordinate bismuth(III) complexes with 2-acetylthiophene thiosemicarbazones: synthesis, characterization, and biological properties. *New J Chem*; 47: 12779-12789.

[17]. Almeida, JCL, Amim, RS, Pessoa, C, Lourenço, MCS, Mendes, IC, Lessa, JA. 2020. Bismuth(III) complexes with pyrazineformamide thiosemicarbazones: investigation on the antimicrobial and cytotoxic effects. *Polyhedron*; 189: 114709.

[18]. Wu, R, He, J, Lin, Q. 2025. Two bismuth-mercapto one-dimensional coordination polymers with efficient visible light-driven catalysis. *J Solid State Chem*; 346: 125272.

[19]. Rajasekharan-Nair, R, Moore, D, Kennedy, AR, Reglinski, J, Spicer, MD. 2014. The stability of mercaptobenzothiazole based soft scorpionate. *Inorg Chem*; 53: 10276-10282.

[20]. Jagenbrein, M, Monakhov, KY, Braunstein, P. 2015. A dinuclear Bi(III) complex of a 1,3-disubstituted imidazole-2-thione and its use as a transmetallation agent toward Pd(II). *J Organomet Chem*; 796: 11-16.

[21]. Ucar, O, Grześkiewicz, AM, Banti, C, Hadjikakou, SK, Ozturk, II. 2021. Structural characterization and biological evaluation of antimony(III) and bismuth(III) complexes with imidazolidine-2-thione. *J Mol Struct*; 1235: 130270.

[22]. Ozturk, II, Sirinkaya, ET, Cakmak, M, Gürgan, M, Ceyhan, D, Panagiotou, N, Tasiopoulos, AJ. 2021. Structural and biological features of bismuth(III) halide complexes with heterocyclic thioamides. *J Mol Struct*; 1227: 129730.

[23]. Cakmak, M, Ozturk, II, Banti, CN, Manoli, M, Moushi, E, Tasiopoulos, AJ, Grzeskiewicz, AM, Kubicki, M, Hadjikakou, SK. 2018. Bismuth(III) bromide-thioamide complexes: synthesis, characterization and cytotoxic properties. *Main Gr Met Chem*; 41: 143-154.

[24]. Yarar, S, Ozturk, II, Banti, CN, Panagiotou, N, Papatriantafyllopoulou, C, Manoli, M, Manos, MJ, Tasiopoulos, AJ, Hadjikakou, SK. 2018. Synthesis, characterization and cytotoxic properties of bismuth(III) chloride complexes with heterocyclic thioamides. *Inorgan Chim Acta*; 471: 23-33.

[25]. Ozturk, II, Banti, CN, Hadjikakou, SK, Panagiotou, N, Tasiopoulos, AJ. 2019. Structural architectures and biological properties of main group bismuth(III) iodide complexes with heterocyclic thioamides. *Inorgan Chim Acta*; 497: 119094.

[26]. Uçar, O. 2025. Theoretical structural studies of transition metal complexes of Schiff base ligands containing ferrocene and imidazole moieties. *ADU J Sci Eng*; 2: 14-21.

[27]. Akintemi, EO, Govender, KK, Singh, T. 2022. A DFT study of the chemical reactivity properties, spectroscopy and bioactivity scores of bioactive flavonols. *Comput Theor Chem*; 1210: 113658.

[28]. Sharma, N, Singh, HL. 2025. Spectroscopic, DFT, antibacterial, and in silico investigations of novel semicarbazone and thiosemicarbazone synthesised from asymmetrical chalcones. *Next Mater*; 7: 100511.

[29]. Bhattacharjee, T, Nath, S, Sen, T, Nethaji, K, Farhana, A, Roy, S, Baildya, N, Gannon, PM, Kaminsky, W, Banerjee, A, Shanmugam, P, Gargari, MS, Pathak, S, Adhikari, S. 2025. A neutral 1D polymeric Hg(II) complex harvested from 9-butyl adenine: synthesis, crystal structure, Hirshfeld surface, DFT optimization, and anti-microbial activities. *J Mol Struct*; 1339: 142389.

[30]. Kumhar, D, Patel, RN, Patel, SK, Patel, AK, Patel, N, Butcher, RJ. 2022. Structural diversity of copper(II) complexes with three dimensional network: crystal structure, Hirshfeld surface analysis, DFT calculations and catalytic activity. *Polyhedron*; 214: 115633.

[31]. Un, Z, Javed, R, Ahmad, A, Qabil, A, Aldamen, MA, Qabil, A, Ibragimov, AB, Nadeem, M. 2026. Triethanolamine-based Cd(II) complex with unusual coordination number: synthesis, characterization, Hirshfeld surface analysis and photocatalytic degradation of organic dyes. *J Mol Struct*; 1356: 145064.